Revisiting iterative time reversal processing: Application to detection of multiple targets

Gabriel Montaldo,[a] Mickaël Tanter, and Mathias Fink
Laboratoire Ondes et Acoustique, ESPCI, Université Paris VII, U.M.R. C.N.R.S. 7587, 10 rue Vauquelin, 75005 Paris, France

(Received 4 October 2002; accepted for publication 30 October 2003)

The iterative time reversal processing represents a high speed and easy way to self-focus on the strongest scatterer in a multitarget medium. However, finding weaker scatterers is a more difficult task that can be solved by computing the eigenvalue and eigenvector decomposition of the time reversal operator, the so-called DORT method. Nevertheless, as it requires the measurement of the complete interelements response matrix and time-consuming computation, the separation of multiple targets may not be achieved in real time. In this study, a new real time technique is proposed for multitarget selective focusing that does not require the experimental acquisition of the time reversal operator. This technique achieves the operator decomposition using a particular sequence of filtered waves propagation instead of computational power. Due to its simplicity of implementation, this iterative process can be achieved in real time. This high speed selective focusing is experimentally demonstrated by detecting targets through a heterogeneous medium and in a speckle environment. A theoretical analysis compares this technique to the DORT formalism.
 [DOI: 10.1121/1.1636463]

PACS numbers: 43.60.Pt, 43.40.Fz, 43.60.Cg [RLW] Pages: 776–784

I. INTRODUCTION

Over the past decade, acoustic time reversal mirrors[1–3] (TRMs) have been studied widely in medical imaging,[4,5] nondestructive testing,[6] and underwater acoustics.[7,8] An extensive overview of TRM applications can be found in Ref. 9. A time reversal mirror is an array of transducers able to work both in transmitting and receiving mode. When a TRM receives the signal coming from an acoustic source or reflector, it time-reverses the received signals and re-emits them into the medium. The resulting wave front focuses back on the acoustic source or reflector location. When the medium contains several reflectors, the time reversal process can be iterated in order to focus on the brightest target as demonstrated in Refs. 10 and 11 in ultrasonic acoustic laboratory experiments and by Kuperman *et al.* in underwater acoustics.[8,12] The potential of such an iterative time reversal processing was also demonstrated experimentally for medical applications by achieving real time tracking of kidney stones in lithotripsy treatments.[4]

The main limitations of the iterative time reversal process are the impossibility of finding weaker targets and the progressive monochromatization of the signals. At each illumination and reception the signals' bandwidth is narrowed by the limited bandpass of the transducers. Thus, after some iterations, the transmitted and received signals become almost monochromatic.

In order to achieve selective detection and focusing on each scatterer inside an unknown multitarget medium, another approach was developed by Prada *et al.* As is demonstrated in Ref. 13, the echoes of a single target are an eigenvector of the time reversal operator. Using this basic idea that each target is associated to an eigenvector of the time reversal operator it is possible to record the whole time reversal operator and compute its eigenvector decomposition. Thanks to this numerical eigenvector decomposition, a selective focusing on each target can be achieved. Using this technique, known as the DORT method,[13–15] Chambers *et al.* have shown that the spectrum of the time reversal operator can be complex and very informative.[16] However, the DORT method is not a real time method because it requires the measurement of the N×N interelement impulse responses and the computation of the eigenvectors decomposition is quite time consuming.

Recently, Kim *et al.*[17,18] have found an elegant way to detect multiple targets in an underwater waveguide without requiring experimental acquisition of the time reversal operator. The basic idea is first to iterate the time reversal process in order to learn how to focus on the strongest scatterer. Then an algorithm of variance minimization based on the inversion of the cross-spectral density matrix allows one to know how to steer a null on this point. This set of signals avoids any reverberation at the strongest target location and thus can be used to focus on the secondary targets. The second brightest target is then selected by iterating the time reversal process. The prior advantage of this nulling method is that it does not require the fastidious acquisition of the time reversal operator. However, it suffers the same limitation as the iterative time reversal processing: The emission signals' bandwidth is narrowed after each iteration resulting in almost monochromatic signals at the end of the process. Finally, it requires the numerical inversion of the cross-section density matrix. The detection of targets presenting important weight differences is limited by the fact that the strongest

[a]Author to whom all correspondence should be addressed; electronic mail: gabrielmontaldo@yahoo.fr

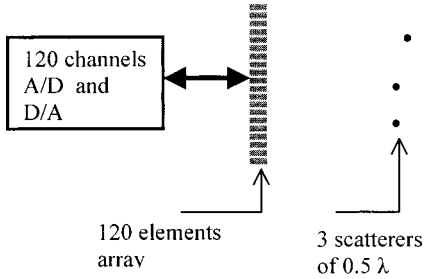

FIG. 1. Configuration of the example. The TRM is composed of an array of 120 elements and a multichannel electronic able to send fully programmable wave forms and record the backscattered echoes. Three targets were embedded in the medium for this example.

target picks up the energy focused on weaker targets and finishes by dominating after some iterations.

In this article, we propose a new real time technique for multitarget selective focusing that does not require the experimental acquisition of the time reversal operator and its numerical decomposition. This technique achieves the operator decomposition simply by using a particular sequence of filtered waves instead of computational power. The general idea of this new approach is to use the time reversal iterative process in order to focus on the brightest target. These signals are then used to derive a broadband cancellation filter which allows one to cancel the echoes of the found target. The selection of the next brightest target is done by iterating the time reversal plus the cancellation filter. This process can be extended to the following of multiple targets detection using the cancellation filter that cleans up the targets already detected. The drawback of temporal spreading induced during the iterative time reversal selection is also overcome by introducing a ''pulse compression operator.'' This operator uses the spread signals coming from the iteration to reconstruct a set of sharp pulsed signals focusing on the selected target.

In Sec. II, the basic principles of the process are explained and illustrated with some preliminary experimental results. In Sec. III, the theoretical formalism of the method is presented and its similarities with the DORT method are highlighted. In Sec. IV, the process is applied to detecting in real time several scatterers through an aberrating medium but also in a noisy ''speckle environment'' as is the case in medical imaging.

II. THE ITERATIVE DECOMPOSITION

In order to explain the iterative decomposition method, we consider a simple homogeneous medium containing three scatterers made with a steel wire of 0.4 mm diameter.

The experiments are conducted in the ultrasonic range in a water tank. The acoustic waves are emitted and received with a standard linear array made of 120 elements working at a 1.5 MHz central frequency. This array is connected to a multichannel system made of 120 independent electronic channels containing A/D and D/A converters (50 MHz sampling, 20 MHz bandwidth). We acquire the signals in a window of 25 μs. The experimental setup is presented in Fig. 1.

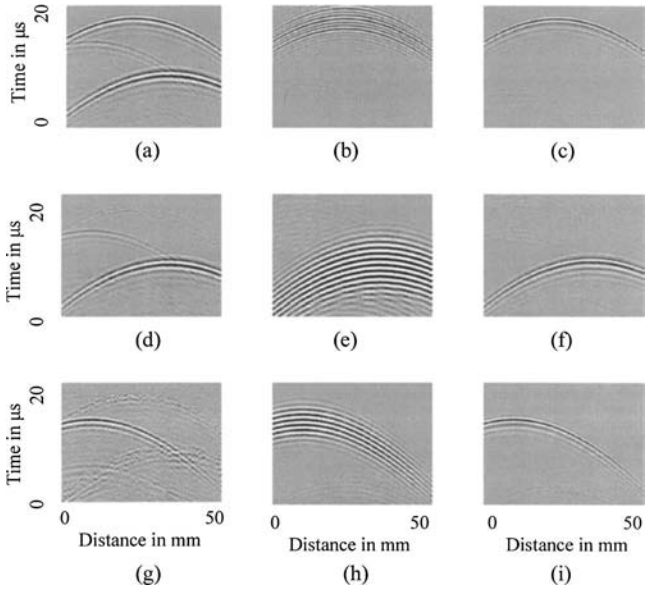

FIG. 2. The iterative process. (a) Backscattered echoes of the three scatterers after a plane wave emission. (b) Detection of the strongest scatterer by iterative time reversal. (c) Eigenpulse of the first scatterer. (d) Backscattered echoes of the two scatterers after filtering the first one. (e) Detection of the second scatterer by time reversal and filtering. (f) Eigenpulse of the second scatterer. (g) Signal of the third scatterer after filtering the first and second one. (h) Detection of the third scatterer by time reversal and filtering. (i) Eigenpulse of the third scatterer.

The process identifies each target step by step beginning from the most reflective one to the weakest one. The selective identification of a new target is made in three steps.

A. First step: Time-reversal processing

A plane wave is emitted in this medium. The backscattered signals are composed of three wave fronts of different amplitudes corresponding to each target [Fig. 2(a)]. If these signals are time reversed and reemitted through the medium, the resulting wave fronts focus on each target and the brightest target is more illuminated than the others. Consequently, its contribution in the backscattered echoes is more important. After a few iterations this time-reversal process permits one to select the most reflecting scatterer. However, at each iteration the signals are filtered by the limited bandwidth of the transducers and it results in a progressive temporal spreading of the emission signals. In Fig. 2(b) we can see the received signal after eight iterations of the time-reversal process, the strongest scatterer was selected but the bandwidth was clearly reduced. The second step of the process allows one to overcome this problem.

B. Second step: Building an "eigenpulse" signal by pulse compression

The bandwidth narrowing suffered during the time reversal process is a real drawback in most applications. An easy solution consists in reconstructing a wideband wave front at each iteration by detecting the arrival time and amplitude law of the signals received on each transducer. The arrival time and amplitude law is then used to reemit a wideband pulsed signal identical on each transducer with the corresponding amplitudes and time delays on each of them. It

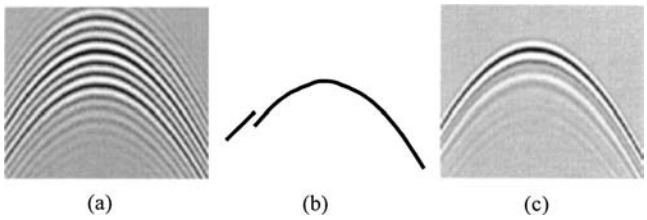

FIG. 3. (a) After the iteration of the time reversal process the signal is spread in time. (b) Selection of a wave front. Using a simple algorithm it has a defect. (c) After emitting this wave front, we obtain a narrow pulse without defects in the identification of the wave front.

allows one to avoid the bandwidth spreading of the signals during the iterative process. The arrival time and amplitude can be measured by using a simple maximum detection technique for each transducer (see Fig. 3). In general, the use of a simple algorithm for the ''pulsed wave front'' construction (for example, a maximum detection) can induce some errors in the arrival time estimation. For example, if the signal is composed of several sinusoids as presented in Fig. 3(a) the maximum detection can be limited by a 2π uncertainty [Fig. 2(b)]. It results in the reemission of an incorrect wave front at the next illumination. However, most of the energy of this incorrect wave front is focused on the good location and the maximum detection on the next backscattered echoes becomes easier and more accurate. Thus, a few iterations of the time reversal process combined with the pulse compression allow one to obtain a correct pulsed wave front or ''eigenpulse'' signal [Figs. 3(c) and 2(c)].

In most of our configurations this part of the process was not critical to the convergence of the method. Even if the maximum detection at the first iteration does not give the good wave front [i.e., it has a lot of ''phase gaps'' as in Fig. 3(b)], after the emission of this incorrect wave front a nonnegligible part of the energy focuses on the target and the backscattered echoes are short pulses for which the maximum detection gives a better wave front.

C. Third step: Canceling the detected scatterer and selecting a new one

The basic idea for selecting a new scatterer is to apply a ''cancellation operator'' able to clear up all the signals coming from the previous detected target. The details of this operator will be explained in Sec. III. If we start with a backscattered signal containing the echoes of the three scatterers [Fig. 2(a)], after applying the cancellation operator we obtain the filtered signals shown in Fig. 2(d). As we can see, the echoes of the strongest scatterer have been canceled. This new set of filtered signals is now used as initial illumination for the iterative time reversal process. The cancellation filter is applied at each step during the iterative time reversal process proposed in Secs. II A and II B. Consequently the first target is not illuminated, the second target generates the brightest echoes and it is progressively selected by the iteration process [Fig. 2(e)].

The signals backscattered by the second target are temporally spread and can be ''pulse compressed'' as described in Sec. II B [Fig. 2(f)]. Finally, the cancellation filter permits one to cancel the first and second targets and selects the third target by iterating the time reversal process. Figures 2(g)–(i) describe the final eigenvector decomposition that was found for the third and weakest target.

The complete process does not require any hard numerical computation, the cancellation and pulse compression operators are easy to calculate, and the combination of steps II B and II C was found sufficient to select multiple targets. The speed of detection is directly linked to the traveling time of the waves in the medium. For short distances as in the human body, this method can be implemented for real time selective focusing. For example with a propagation distance of 15 cm a step of iterative time reversal process takes only 1 ms, the maximum detection and the cancellation filter can be done in 3 ms. Running the complete detection of the three targets of Fig. 1 takes nearly 50 ms. With this short time of detection it is possible to track moving multiple targets.

We will demonstrate experimentally in Sec. IV that this process is robust not only in a noisy environment (like speckle noise for medical applications) but also through an aberrating medium. For this purpose, this technique can also be seen as a phase aberration correction technique using the bright spots embedded in the medium.

III. THEORETICAL APPROACH

A. The iteration of the time reversal

We consider a system composed of an array of transducers capable of working both in transmitting and receiving mode and a linear medium of propagation containing a few point-like scatterers. The propagation medium is heterogeneous but we suppose that the amplitude and phase perturbation are not very different for different frequencies (i.e., strongly dispersive media will not be considered).

The signals received and emitted by the transducers array are functions of space and time $e=e(x,t)$, where x denotes the different positions of the individual transducers.

A complete time reversal iteration has two steps: first, a signal $e=e(x,t)$ is emitted and the echoes backscattered by the medium $r=r(x,t)$ are recorded by the array. Second, these signals are time reversed $r(x,-t)$ and they are reemitted by the array. The backscattered echoes are recorded by the array and correspond to the first set of iterated signals $e^{(1)}=e^{(1)}(x,t)$. The original set of signals and its first iteration are related by the time reversal operator of the medium $\mathbf{H}$ and can be written in a compact form

$$e^{(1)}=\mathbf{H}e. \tag{1}$$

Note that $\mathbf{H}$ denotes the application of a spatiotemporal linear operator to the signals $e(x,t)$. The notation H will refer to the matrix representation of this operator. The eigenmodes of this time reversal operator $\mathbf{H}$ are a set of signals $\nu_i=\nu_i(x,t)$ that verify $\mathbf{H}\nu_i=\lambda_i\nu_i$, where λ_i is the associated eigenvalue. In a free space medium with some punctual targets, the eigenvectors are monochromatic cylindrical waves focused on the targets. Assuming that the sound speed and absorption heterogeneities are due to a random screen located closed to the array, it introduces only different amplitude gains and time delays on each transducer of the array. Then the eigenmodes can be written as

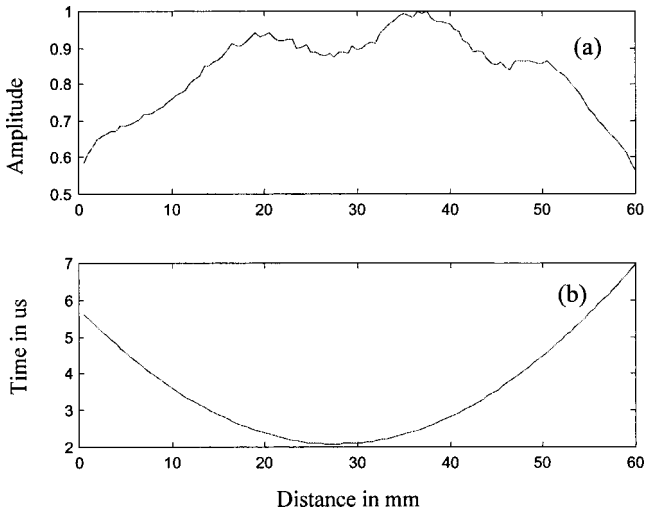

FIG. 4. (a) Amplitude $A(x)$ and delay $\tau(x)$ for the first scatterer of Fig. 1.

$$\nu_{i\omega}(x,t)=A_i(x)\exp(j\omega[t+\tau_i(x)]), \tag{2}$$

where $\tau_i(x)$ is a time delay law depending only on the scatterer location and medium aberrations and $A_i(x)$ is the amplitude of the signal coming from the scatterer and received on the transducer located at x. $A_i(x)$ and $\tau_i(x)$ describe completely the eigenmode associated with scatterer i. As an example, Fig. 4 represents the experimental amplitude and time delay law associated with the first target corresponding to the Fig. 1 setup. An eigenmode associated with this particular target at 1 MHz frequency is presented in Fig. 5.

Note that the eigenmodes $\nu_{i\omega}(x,t)$ and their eigenvalues $\lambda_{i\omega}$ must validate

$$\mathbf{H}\nu_{i\omega}=\lambda_{i\omega}\nu_{i\omega}, \tag{3}$$

and the orthogonal relationship

$$\int\int \nu^*_{i\omega}(x,t)\nu_{j\omega'}(x,t)dx\,dt=\delta_{ij}\delta_{\omega\omega'}. \tag{4}$$

We can build a matrix representation of the time reversal operator in the base of the spatiotemporal eigenmodes as

$$H_{i\omega,j\omega'}=\int\int \nu^*_{i\omega}(x,t)\mathbf{H}\nu_{j\omega'}(x,t)dx\,dt. \tag{5}$$

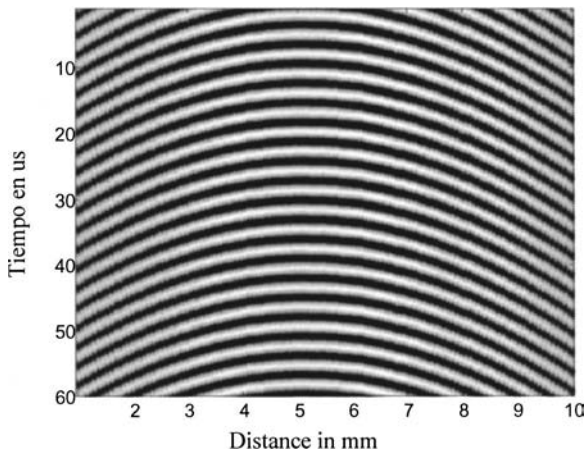

FIG. 5. Eigenmode of the first scatterer for a frequency of 1 MHz.

This matrix is diagonal and contains the eigenvalues $\lambda_{i\omega}$. If we rank the pairs of index i, ω first by the scatterer index i and after by its frequency ω, we can see this matrix in a graphical representation as

$$H_{i\omega,j\omega'}=\begin{bmatrix} \lambda_{11} & \cdot & \cdot & 0 \\ & \lambda_{1\ldots} & & \\ & & \lambda_{1n} & \\ & & & \lambda_{21} \\ & & \lambda_{2\ldots} & \\ 0 & & & \lambda_{2n} \end{bmatrix} \tag{6}$$

In this case we assumed that there are only two scatterers in the medium. Using this representation of the time reversal operator, it is easy to see what happens in an iteration of the time reversal process. We start with an arbitrary excitation $e(x,t)$ and decompose it in the eigenvector base

$$e(x,t)=\sum_{i\omega} e_{i\omega}\nu_{i\omega}(x,t), \tag{7}$$

where $e_{i\omega}$ are the weights of each eigenvector. After applying the time reversal operator, the new coefficients of the signals are $e^{(1)}_{i\omega}=\lambda_{i\omega}e_{i\omega}$ and after n iterations the coefficients become $e^{(n)}_{i\omega}=\lambda^n_{i\omega}e_{i\omega}$. After each iteration, the coefficient of the strongest eigenvalue is strengthened in comparison to the secondary scatterers and the time reversal converges toward the eigenmode corresponding to the strongest eigenvalue.

As the response of the transducer and the cross section of the scatterers depend on the frequency, $\lambda_{i\omega}$ has different values for different frequencies. After each iteration, the coefficient of the strongest eigenvalue is strengthened and the time reversal converges toward the eigenmode corresponding to the strongest eigenvalue. Experimentally, the bandwidth of the signal is narrowed at each step of the iterative process and the signal spreads in time.[19]

B. Iteration with an intermediate operator

As was previously seen, the iterative time reversal permits one to identify the brightest scatterer embedded in a medium but it presents some inconveniences. First, it is not possible to find weaker targets. Second, as the eigenvectors are monochromatic waves, the iterative time reversal expands the length of the signals and it is not possible to apply a large number of iterations. A modification of the time reversal process is introduced to overcome these limitations. The main idea is to apply an intermediate operator $\mathbf{O}$ after each iteration of the time reversal process. Thus, if we start with a set of emission signals $e(x,t)$, the new set of signals after the iteration will be

$$e^{(1)}=\mathbf{HO}e=\tilde{\mathbf{H}}e, \tag{8}$$

where $\tilde{\mathbf{H}}=\mathbf{HO}$ is the effective iteration operator. We can define the matrix representation of $\mathbf{O}$ in the base of eigenvectors of $\mathbf{H}$ in a similar manner to Eq. (5),

$$O_{i\omega,j\omega'}=\int\int \nu^*_{i\omega}(x,t)\mathbf{O}\nu_{j\omega'}(x,t)dx\,dt, \tag{9}$$

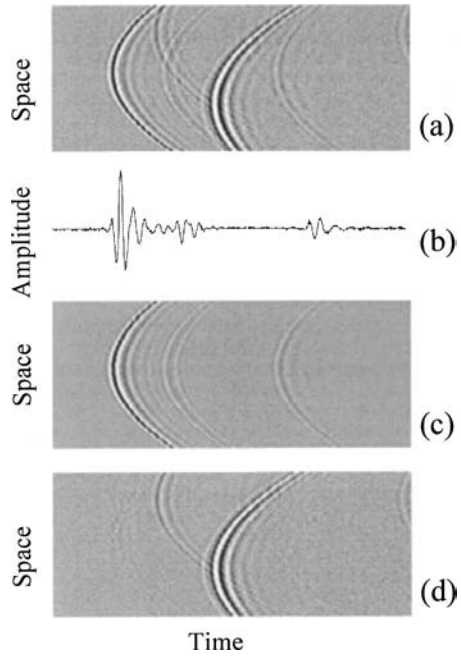

FIG. 6. Illustration of the filter operator. From the original image (a) we calculate the weight of the first scatterer at each instant with Eq. 13(b). Performing the convolution of this weight with the wave front function we obtain the echoes of the first scatterer (c). Subtracting (c) from (a) we obtain the echoes of the other scatters (d).

Decomposing the signal $e(x,t)$ as in Eq. (7) it is easy to calculate that the coefficients $e_{i\omega}^{(1)}$ after the iteration are

$$e_{i\omega}^{(1)} = \sum_{j\omega'} \tilde{H}_{i\omega,j\omega'} e_{j\omega'}, \tag{10}$$

where

$$\tilde{H}_{i\omega,j\omega'} = \sum_{k\omega''} H_{i\omega,k\omega''} O_{k\omega'',j\omega'}. \tag{11}$$

An eigenvector $b_{i\omega}$ of the $\tilde{H}_{i\omega,j\omega'}$ matrix associated with an eigenvalue β verifies $\Sigma_{j\omega'} \tilde{H}_{i\omega,j\omega'} b_{j\omega'} = \beta b_{i\omega}$. After iterating n times, the process amplifies β^n times this eigenvector. The strongest eigenvalue is finally selected after some iterations of Eq. (10). The use of an adequate operator **O** allows us to transform the convergence of the time reversal process from the strongest eigenvalue of **H** to the strongest eigenvalue of $\tilde{\mathbf{H}}$.

C. The cancellation operator

This operator solves the first problem of finding weaker scatterers in a multitarget environment, it permits one to clean the echoes of a brighter scatterer previously detected in order to find the next one.

The calculus of this operator starts with the knowledge of the time delay $\tau_i(x)$ and the amplitude $A_i(x)$ of the scatterer, with these data we can build a ''wave form function'' as

$$w_1(x,t) = \delta[t + \tau_1(x)] A_1(x). \tag{12}$$

where δ is the Dirac's function. In this example we chose the wave form function for the first scatterer.

If we have a signal $e(x,t)$, we can build a function $P(t)$ that gives the weight of the echoes of the first scatterer in the signal at each time as

$$P(t) = \int \int e(x',t') w_1(x',t'-t) dt'\, dx'$$
$$= \int e[x', t - \tau_1(x')] A_1(x') dx'. \tag{13}$$

At each time t, the multiplication by the wave form function selects the echoes of the first scatterer at time t. Performing the integration we obtain an amplitude of the echoes of the first scatterer [Fig. 6(b)].

With the amplitude we can rebuild the echoes of the first scatterer performing the correlation between $P(t)$ and the wave form function [see Fig. 6(c)],

$$\int P(t') w_1(x, t-t') dt' = A_1(x) P[t + \tau_1(x)]. \tag{14}$$

Substituting $P(t)$ by Eq. (13), the echoes of the first scatterer are

$$A_1(x) \int A_1(x') e[x', t + \tau_1(x) - \tau_1(x')] dx'.$$

Finally we subtract these echoes from the signal $e(x,t)$ to obtain one without echoes from the first scatterer [Fig. 6(d)]. As a conclusion the cancelation operator is

$$\mathbf{F}^1 e(x,t) = e(x,t) - A_1(x) \int A_1(x') e[x', t + \tau_1(x) - \tau_1(x')] dx'. \tag{15}$$

Calculating the elements of this operator with the matrix formalism introduced in Eq. (9), we obtain

$$F^1_{i\omega,j\omega'} = (1 - \delta_{1i}) \delta_{ij} \delta_{\omega\omega'}. \tag{16}$$

The complete deduction of Eq. (16) is given in the appendix. Note that the diagonal elements of the matrix defined in Eq. (16) are equal to 1 except for all the frequency components of the first target which are equal to zero. After multiplying by the diagonal matrix $H_{i\omega,j\omega'}$, we obtain the matrix representation of the operator $\mathbf{HF}^1$,

$$HF^1=\begin{bmatrix}\lambda_{11} & \cdot & \cdot & 0\\ & \lambda_{1\ldots} & & \\ & & \lambda_{1n} & \\ & & & \lambda_{21}\\ & & & & \lambda_{2\ldots}\\ 0 & & & & & \lambda_{2n}\end{bmatrix}\times\begin{bmatrix}0 & & & & & 0\\ & 0 & & & & \\ & & 0 & & & \\ & & & 1 & & \\ & & & & 1 & \\ 0 & & & & & 1\end{bmatrix}=\begin{bmatrix}0 & & & & & 0\\ & 0 & & & & \\ & & 0 & & & \\ & & & \lambda_{21} & & \\ & & & & \lambda_{2\ldots} & \\ 0 & & & & & \lambda_{2n}\end{bmatrix}.$$

Due to the cancellation of the diagonal values of the first eigenvector, the second scatterer presents the strongest eigenvalue in HF^1, and iterating the operator $\mathbf{HF}^1$, it will converge to the second brightest scatterer.

D. The pulse compression operator

One problem of the iteration with the time reversal is that the signals are enlarged in each iteration. In Sec. II B we proposed to send only one wave front in order to compress the signals. The wave front can be described by the function (12). We can estimate the time delay $\tau_i(x)$ and the amplitude $A_i(x)$ using a maximum detection at each point x. With these estimates it is possible to build a contracting filter that generates a wave front multiplied by the weight depending on the signal $e(x,t)$ as

$$\mathbf{M}^1 e(x,t)=w_1(x,t)\int\int w_1(x',t')e(x',t')dx'\,dt'. \tag{17}$$

The integral $\int\int w_1(x',t')e(x',t')dx'dt'$ gives the weight of the wave front in the signal $e(x,t)$ at time $t=0$ as in Eq. (13).

After performing the integration and substituting $w_1(x,t)$ by Eq. (12) we arrived at a simple expression for the contracting operator,

$$\mathbf{M}^1 e(x,t)=A_1(x)\,\delta[t+\tau_1(x)]\times\int A_1(x')e[x',-\tau_1(x')]dx'. \tag{18}$$

Calculating the projected matrix for this operator as in Eq. (9) we obtain

$$M^1_{i\omega j\omega'}=\delta_{1i}\delta_{1j}1_{\omega\omega'}, \tag{19}$$

where $1_{\omega,\omega'}$ is a matrix of 1 for all values of ω and ω'. The complete calculus of Eq. (19) is given in the appendix. This operator can be seen as a mask set to 1 in a square corresponding to all frequency components of the first scatterer and 0 elsewhere. After the multiplication of the mask matrix by the diagonal matrix $H_{i\omega,j\omega'}$, we obtain the matrix representation of the operator $\mathbf{HM}^1$,

$$HM^1=\begin{bmatrix}\lambda_{11} & \cdot & \cdot & 0\\ & \lambda_{12} & & \\ & & \lambda_{13} & \\ & & & \lambda_{21}\\ & & & & \lambda_{22}\\ 0 & & & & & \lambda_{23}\end{bmatrix}\times\begin{bmatrix}1&1&1&0&\cdot&0\\1&1&1&0&\cdot&\cdot\\1&1&1&0&\cdot&\cdot\\0&0&0&0&\cdot&\cdot\\ \cdot&\cdot&\cdot&\cdot&0&\cdot\\0&\cdot&0&\cdot&\cdot&0\end{bmatrix}=\begin{bmatrix}\lambda_{11}&\lambda_{11}&\lambda_{11}&0&\cdot&0\\\lambda_{12}&\lambda_{12}&\lambda_{12}&0&\cdot&\cdot\\\lambda_{13}&\lambda_{13}&\lambda_{13}&0&\cdot&\cdot\\0&0&0&0&\cdot&\cdot\\ \cdot&\cdot&\cdot&\cdot&0&\cdot\\0&\cdot&0&\cdot&\cdot&0\end{bmatrix}.$$

The eigenvector of highest eigenvalue is $(\lambda_{11},\lambda_{1,\ldots},\lambda_{1n},0,\ldots,0)$ and its eigenvalue is

$$\tilde{\lambda}_i=\sum_{\omega}\lambda_{i\omega}. \tag{20}$$

In conclusion, the compression operator allows one to select all the frequency components of a same scatterer and add them. As all the frequency components are summed the

TABLE I. Scheme of the applied operators and their function.

Step	Operator	Action
1	H^n	After n iterations of time reversal processing, the first target is selected. τ_1 and A_1 are estimated.
2	HM^1	Building the first "eigenpulse." τ_1 and A_1 are then reevaluated.
3	$(HF^1)^n$	Filtering the first target, the second becomes the strongest. τ_2 and A_2 are estimated after n iterations.
4	$(HF^1)^nM^2$	Building the second eigenpulse. τ_2 and A_2 are reevaluated.
5	$(HF^2F^1)^n$	Filtering the first and second scatter. The third becomes the strongest. τ_3 and A_3 are estimated after n iterations.
6	$(HF^2F^1)^nM^3$	Building the third eigenpulse. τ_3 and A_3 are reevaluated.
7	$(HF^3F^2F^1)^n$	Filtering the first, second, and third targets. The fourth becomes the strongest ...

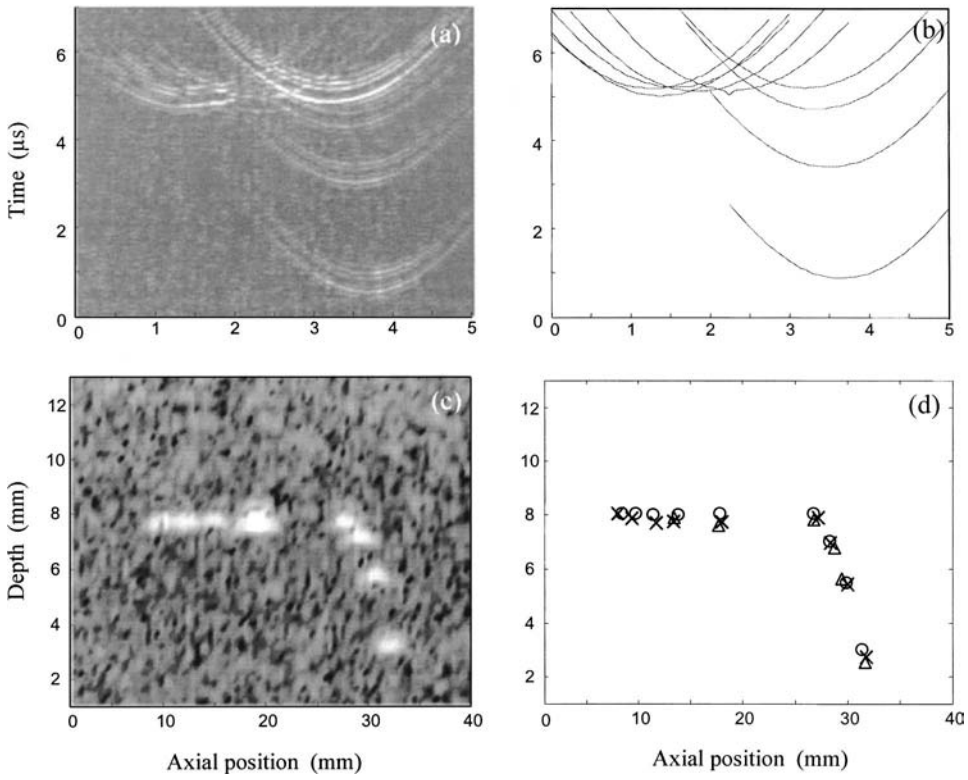

FIG. 7. Target detection in a biological phantom. (a) Signal received after a plane wave illumination, we can see some echoes of the target with an important noise of the structure of the phantom. (b) Detection of the echoes of the nine targets. (c) Echographic image of the phantom due to the speckle noise. The first three targets are difficult to resolve. (d) Calculation of the target position from the detected echoes. Crosses are the measured positions, the circles are given by the furnisher of the phantom, and the triangles are the positions calculated from the maximum of the *B* scan. The maximum detection in the *B* scan is not able to give the positions and number of scatters for the first three scatterers well.

temporal spreading is avoided and a narrow pulse that focuses on the target is possible to obtain.

This technique is similar to applying an inverse filter to compensate the bandwidth of the transducer. However, such an inverse filter is more sensitive to noise, needs a precalibration of the transducers and lots of calculations that limit the real-time aspect of the technique. Extending these two operators $\mathbf{F}^1$ and $\mathbf{M}^1$ to other targets we obtain two sets of operators: the filter operators $\mathbf{F}^i$ which cancel the echoes of the ith scatterer and the pulse compression operators $\mathbf{M}^i$ which compact the echoes of scatterer i in a narrow pulsed signal. These two kinds of operators are used to detect all the targets successively as summarized in Table I. As a final observation, this system has some similitude with the DORT method.

The DORT method starts with the measurement of the interelement response matrix. This matrix is a representation of the time reversal operator **H**. Performing a numerical decomposition of this matrix we obtain the complete set of eigenmodes $\nu_{i\omega}(x,t)$. Adding all the eigenmodes ω of a same target i we can build a pulse that focuses on the target as $\nu_i(x,t)=\Sigma_\omega \nu_{i\omega}(x,t)$.

However, in the DORT method the decomposition is achieved frequency by frequency and an eigenpulse can be built by recombining the DORT eigenvectors but there is a relative phase ambiguity between eigenvectors of different frequencies. This problem makes the recombination of the eigenvectors nonunique.

This final result is similar to the ''eigenpulses'' obtained by the iterative decomposition but substituting the numerical calculation by a specific convergence of the time reversal process over each target.

IV. EXAMPLES OF DETECTION IN INHOMOGENEOUS MEDIA

The most interesting applications of multitarget detection correspond to inhomogeneous media. If the phase and amplitude aberration are not extremely hard we are in the hypotheses that $\tau_i(x)$ and $A_i(x)$ are independent of the frequency and this method is able to detect the targets.

The first application is to find nine nylon wires of half wavelength diameter (0.4 mm) in a biological phantom with an important ''speckle noise'' structure.

Figure 7(a) shows the echoes of the phantom when it is illuminated with a plane wave. We can see the echoes of some targets superposed to a structural speckle noise coming from a random distribution of small scatterers. The iterative method is able to identify the nine echoes as is shown in Fig. 7(b).

Due to the speckle noise a standard echographical image is not able to resolve the first three scatterers of the left-hand side of the image [Fig. 7(c)]. Using the time delays detected

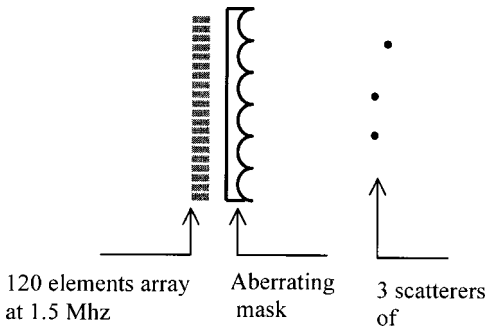

FIG. 8. Identification through an aberrating mask.

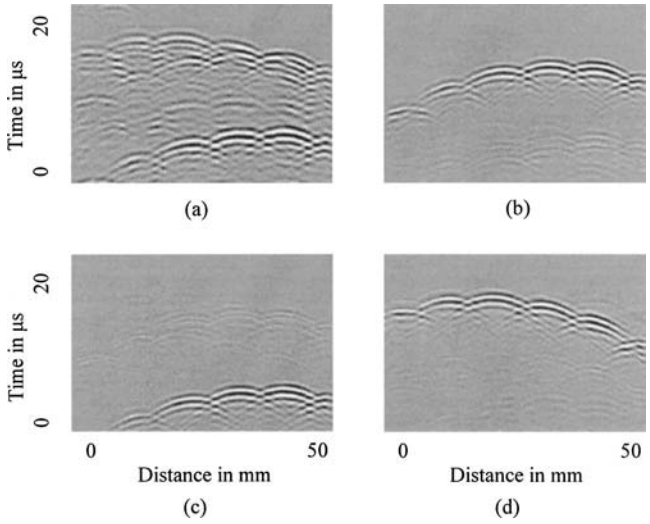

FIG. 9. Identification of three scatterers through an aberrating mask. (a) Echoes of the three scatters after a plane wave excitation. (b), (c), and (d) Identification of the three scatters.

by the iterative method we can calculate the position of each scatterer. Figure 7(d) shows the calculated positions, the positions given by the furnisher and the ones obtained taking the maximum of the *B* scan of Fig. 7(c).

The maximum detection in the *B*-scan image can be applied to the last six scatterers where the resolution is enough to isolate each target. However, for the first three scatterers it is impossible to give the good number of targets and their respective positions directly from the classical *B*-scan image.

A possible application could be the identification of microcalcifications in the breast, if a suspicious area is detected by a conventional image, an automatic detection of punctual scatterers could give extra information to detect the calcifications.

The final experience consisted in putting an aberrating mask between the array and the scatterers. The mask is made of a soft polymer composed of semicircles of 1 cm each, the scatterers are the same as in the experiment of Fig. 1 (see Fig. 8). Figure 9(a) shows the echoes of three scatterers when we insonify them with a plane wave.

In Fig. 10 we can see the *B* scan of the three scatterers through the aberrating mask. Due to the particular geometry

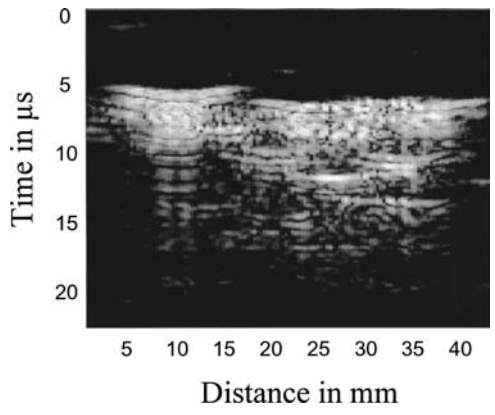

FIG. 10. *B* scan of the scatterers through the mask, there are a lot of ''virtual images'' of the scatters that do not permit to identify the scatters.

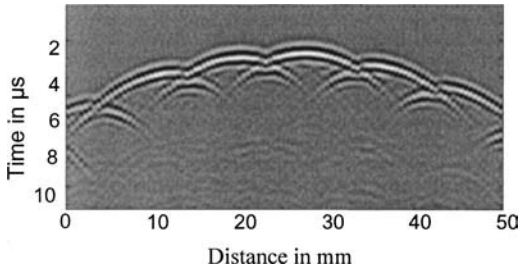

FIG. 11. Simulation of the echo of a single target through the aberrating mask used in the experience of Fig. 9. We can see the resemblance between this simulation and the eigenpulses detected in Fig. 9.

of the mask the *B* scan shows a lot of ''virtual replica'' of the scatterers, and then it is impossible to know how many real scatterers there are in the medium and how to focus on each one.

After the application of the iterative method the three scatterers were identified [Figs. 9(b)–(d)]. The wave fronts are composed of a succession of small arches. We have done a simulation of the aberrator by finite differences in order to verify the form of the eigenmodes. In Fig. 11 we show the simulation of the first scatterer that has the same form as Fig. 9. This last example clearly demonstrates the efficiency of the method in a strongly aberrating medium. These experimental examples show a good stability of the method. A failure of this iterative method was detected when two targets of very different size were located close together. In this case, the cancellation operator is not precise enough to clean up completely the echoes of the strongest target and consequently the detection oscillates between the two targets.

V. CONCLUSION

A new real time technique has been proposed for selective focusing on multiple targets. It is based on the combination of the iterative time reversal process with very simple operations like maximum detection and signal subtraction. This method enables one to find and auto focus in real time on multiple targets using two intermediate operators. The cancellation operator permits one to cancel the echoes coming from targets already detected and the iterative time reversal process achieves the adaptive focusing on a new target. A pulse compression operator based on the use of a maximum detection algorithm serves to overcome the problem of signal temporal spreading induced during the iterative time reversal process. Theoretical similarities with the DORT method have been highlighted. Instead of achieving the eigenvector decomposition using time consuming computational power, the new approach builds it experimentally in real time by simply using wave propagation. This high speed selective focusing technique has a potential application in microcalcification detection in breast, nondestructive testing and underwater acoustics. For all these topics the real time capability could be interesting for tracking moving multiple targets.

APPENDIX

We consider a simplified medium containing only a discrete number of scatterers. The aberrations induced by the medium are assumed to be restricted to an amplitude and time delay law independent of the frequency. This amplitude and time delay law differ from one scatterer to the other. The eigenmodes associated with a target are monochromatic waves with an amplitude and phase perturbation assumed to be constant over the transducer bandwidth,

$$\nu_{i\omega}(x,t)=A_i(x)\exp(j\omega[t+\tau_i(x)]), \tag{A1}$$

where the index i denotes the target number and ω is the frequency of the eigenmode. $\tau_i(x)$ is a time delay depending on the array location of the elements of the array. $A_i(x)$ is the amplitude of the signal received on each spatial point. Thus, $\tau_i(x)$ and $A_i(x)$ fully characterize the wave front coming from the target i. The eigenmodes must validate the orthogonal relationship

$$\int\int \nu^*_{i\omega}(x,t)\,\nu_{j\omega'}(x,t)dx\,dt=\delta_{ij}\delta_{\omega\omega'}. \tag{A2}$$

This calculation introduces a condition between the amplitudes and the time delay

$$\int A_i(x)A_j(x)\exp(j\omega[\tau_j(x)-\tau_i(x)])dx=\delta_{ij}. \tag{A3}$$

With this relation we can calculate the matrix representation of the operators.

1. The cancellation operator

The action of the cancellation operator over a signal $e(x,t)$ was defined in Eq. (15) as

$$\mathbf{F}^1e(x,t)=e(x,t)-A_1(x)\int e[x',t+\tau_1(x)-\tau_1(x')]\times A_1(x')dx'. \tag{A4}$$

When we apply this filter to an eigenmode $\nu_{i\omega}$ and use Eq. (A3) the integral becomes

$$A_1(x)\int \nu_{i\omega}[x',t+\tau_1(x)-\tau_1(x')]A_1(x')dx' = \nu_{i\omega}(x,t)\,\delta_{1i}. \tag{A5}$$

The action of the filter over an eigenvector is

$$\mathbf{F}^1\nu_{i\omega}=(1-\delta_{1i})\,\nu_{i\omega}. \tag{A6}$$

The matrix representation of the $\mathbf{F}$ operator is calculated as

$$F^1_{i\omega,j\omega'}=\int\int \nu^*_{i\omega}(x,t)\mathbf{F}^1\nu_{j\omega}(x,t)dx\,dt. \tag{A7}$$

Using Eq. (A7) and the orthogonal relationship (A2) we obtain

$$F^1_{i\omega,j\omega'}=(1-\delta_{1i})\,\delta_{ij}\delta_{\omega\omega'}. \tag{A8}$$

2. The eigenpulse mask operator

We have defined the action of the mask operator over a signal $e(x,t)$ as

$$\mathbf{M}^1e(x,t)=A_1(x)\,\delta[t+\tau_1(x)]\int A_1(x')\times e[x',-\tau_1(x')]dx'. \tag{A9}$$

Using Eq. (A3), the action over an eigenvector $\nu_{j\omega'}$ is

$$\mathbf{M}^1\nu_{j\omega'}(x,t)=A_1(x)\,\delta[t+\tau_1(x)]\,\delta_{1j}. \tag{A10}$$

The matrix representation is calculated as

$$M^1_{i\omega,j\omega'}=\int\int \nu^*_{i\omega}(x,t)\mathbf{M}^1\nu_{j\omega'}(x,t)dx\,dt, \tag{A11}$$

using the orthogonal relationship (A2) we obtain

$$M^1_{i\omega,j\omega'}=\delta_{1i}\delta_{1j}. \tag{A12}$$

This operator is independent of the frequencies ω and ω'. In order to show this propriety we multiplied Eq. (16) by $1_{\omega\omega'}$.

[1] O. Ikeda, "An image reconstruction algorithm using phase conjugation for diffraction-limited imaging in an inhomogeneous medium," J. Acoust. Soc. Am. **85**, 1602–1606 (1989).
[2] M. Fink, "Time-reversal mirrors," J. Phys. D **26**, 1330–1350 (1993).
[3] M. Fink, "Time reversal of ultrasonic fields. II. Basic Principles," IEEE Trans. Ultrason. Ferroelectr. Freq. Control **39**, 554–566 (1992).
[4] J. L. Thomas, F. Wu, and M. Fink, "Time reversal mirror applied to litotripsy," Ultrason. Imaging **18**, 106–121 (1996).
[5] M. Tanter, J.-L. Thomas, and M. Fink, "Focusing and steering through absorbing and aberating layers: Application to ultrasonic propagation through the skull," J. Acoust. Soc. Am. **103**, 2403–2410 (1998).
[6] N. Chakroun, M. Fink, and F. Wu, "Time reversal processing in ultrasonic non destructive testing," IEEE Trans. Ultrason. Ferroelectr. Freq. Control **42**, 1087–1098 (1995).
[7] D. R. Jackson and D. R. Dowling, "Phase conjugation in underwater acoustics," J. Acoust. Soc. Am. **89**, 171–181 (1991).
[8] W. A. Kuperman, W. S. Hodgkiss, H. C. Song, T. Akal, C. Ferla, and D. R. Jackson, "Phase conjugation in the ocean: Experimental demonstration of an acoustic time reversal mirror," J. Acoust. Soc. Am. **103**, 25–40 (1998).
[9] M. Fink, D. Cassereau, A. Derode, C. Prada, P. Roux, M. Tanter, J. L. Thomas, and F. Wu, "Time-reversed acoustics," Rep. Prog. Phys. **63**, 1933–1995 (2000).
[10] C. Prada, F. Wu, and M. Fink, "The iterative time reversal process: A solution to self-focusing in the pulse echo mode," J. Acoust. Soc. Am. **90**, 1119–1129 (1991).
[11] C. Prada, J. L. Thomas, and M. Fink, "The iterative time reversal process: Analysis of the convergence," J. Acoust. Soc. Am. **97**, 62–71 (1995).
[12] H. C. Song, W. A. Kuperman, and W. S. Hodgkiss, "Iterative time reversal in the ocean," J. Acoust. Soc. Am. **105**, 3176–3184 (1999).
[13] C. Prada and M. Fink, "Eigenmodes of the time reversal operator: A solution to selective focusing in multiple-target media," Wave Motion **20**, 151–163 (1994).
[14] C. Prada, S. Manneville, D. Spoliansky, and M. Fink, "Decomposition of the time reversal operator: Detection and selective focusing on two scatterers," J. Acoust. Soc. Am. **99**, 2067–2076 (1996).
[15] N. Mordant, C. Prada, and M. Fink, "Highly resolved detection and selective focusing in a waveguide using the D.O.R.T. method," J. Acoust. Soc. Am. **105**, 2634–2642 (1999).
[16] D. H. Chambers and A. K. Gautesen, "Time reversal for a single spherical scatterer," J. Acoust. Soc. Am. **109**, 2616–2624 (2001).
[17] J. S. Kim, H. C. Song, and W. A. Kuperman, "Adaptive time reversal mirror," J. Acoust. Soc. Am. **109**, 1817–1825 (2001).
[18] J. S. Kim, W. S. Hodgkiss, W. A. Kuperman, and H. C. Song, "Null-broadening in a waveguide," J. Acoust. Soc. Am. **112**, 189–197 (2002).
[19] M. Cheney, D. Isaacson, and M. Lassas, "Optimal acoustics measurements," SIAM (Soc. Ind. Appl. Math.) J. Appl. Math. **61**, 1628–1647 (2001).